

MOMENTUM SPREAD OF THE 200 MeV LINAC BEAM AT NAL

Shoroku Ohnuma

National Accelerator Laboratory

April 10, 1971

Summary

It is demonstrated by a simple calculation that the momentum spread of the 200 MeV beam from the linac at NAL can be reduced (or increased) by simply changing the rf phase between the last two cavities. The nonlinearity of the phase oscillation in the last cavity is utilized intentionally for this purpose. The lowest value obtainable in this scheme without using a buncher is  $\Delta p/p = \pm 1 \times 10^{-3}$ . This value is rather insensitive to the rf level of the last cavity ( $\geq 60\%$  of the design value) or to the beam intensity ( $\leq 100$  mA). With a single buncher and a somewhat reduced rf level (90% of the design value with the synchronous phase changing from  $-32^\circ$  to  $-20^\circ$ ) in the first cavity, the momentum spread can be further reduced to  $\Delta p/p = \pm 0.7 \times 10^{-3}$ .



### INTRODUCTION

The rf voltage per turn of the booster that is required for an efficient adiabatic trapping depends quadratically on the momentum spread of the injected beam,

$$V(\text{in kV}) \geq 7.7 \times 10^7 (\Delta p/p)^2; \quad \Delta p/p = \text{half width.}$$

Since the voltage program is based on a value of 100 kV at the injection,<sup>1</sup> the momentum spread of the injected beam must be  $\pm 1 \times 10^{-3}$  or less. If one considers the inevitable increase of the momentum spread due to space charge forces<sup>2</sup> introduced in the transport between the linac and the booster (~50 m), the requirement for the output beam from the linac becomes more stringent. The usual practice is to use a debuncher which may turn out to be the only solution for achieving the design intensity in the booster. However, since installation of any debuncher is not planned for the initial operation, it is worthwhile to explore simple means of reducing the momentum spread of the linac output beam.

Momentum spread (or energy spread) in the linac beam is due to a finite acceptance area of the longitudinal (phase-energy) phase space around the synchronous point. If the phase oscillation is linear and the beam is perfectly "matched" to the (linearized) acceptance shape at the injection, the final momentum spread at 200 MeV will be,<sup>3</sup> in the adiabatic approximation,

$$\Delta p/p = \pm 0.4 \times 10^{-4} \text{ per } \pm 1^\circ \text{ initial phase spread.}$$

There are several effects which make the actual spread much greater than this idealized value. Even with bunchers, it is not possible to have a perfectly matched initial beam. Space charge forces and drift spaces between two adjacent cavities contribute to a growing mismatching. Phase motion is far from linear and the filamentation in phase space due to nonlinearity makes the "effective" area of the beam increase. The coupling effect between transverse and longitudinal motion<sup>4</sup> is also responsible for the deterioration of the beam quality. Fortunately, all these effects are serious only at low energies and, after 10-20 MeV, the mismatched beam simply rotates within the acceptance area. A mismatched beam is characterized by a "breathing" of the momentum spread (and the phase spread)<sup>5</sup> with a large amplitude and, depending on the phase of this breathing motion at the end of a linac, one can easily have a large momentum spread. For example, initially unbunched beam (no energy spread at .75 MeV) can have  $\Delta p/p \approx \pm 2.5 \times 10^{-3}$  at 200 MeV (NAL linac, 20-40 mA).

A simple way to control the momentum spread at the end of a multicavity linac is to shift the rf phase of the last cavity relative to the incoming beam. The beam is in the nonlinear region of the phase space and the spread of the phase oscillation frequency in the beam is enhanced. One can utilize this nonlinear characteristic to achieve a partial debunching. For given cavity parameters, the amount of the

phase shift needed depends on the shape of the beam in the phase space at the entrance of that cavity.

### PHASE-ENERGY OSCILLATION

#### Notation

- $W, \phi$  : kinetic energy and phase of each particle  
 $W_s, \phi_s$  : synchronous energy and phase; design value of  $\phi_s = -32^\circ$  in all cavities  
 $\lambda$  : rf wave length = 1.4897 m  
 $E_0$  : average acceleration field  
 $T$  : transit time factor  
 $m_0 c^2$  : proton rest energy  
 $c\beta_s, m_0 c^2 \gamma_s, m_0 c \eta_s$  : velocity, total energy and momentum of the synchronous particle

In the linear, adiabatic approximation, the phase and the energy of a particle along a linac (at a distance  $s$ ) are

$$\Delta\phi \equiv \phi - \phi_s = \sqrt{\alpha S} \cos \left( \int_0^S \omega_\phi(s) ds + \theta_0 \right)$$

$$\Delta W \equiv W - W_s = \sqrt{S/\alpha} \sin \left( \int_0^S \omega_\phi(s) ds + \theta_0 \right) \quad (\theta_0 = \text{const.})$$

The invariant phase space area in  $(\Delta\phi) - (\Delta W)$  space is  $\pi S$  and the oscillation frequency  $\omega_\phi$  and the shape parameter  $\alpha$  are

$$\omega_\phi (\equiv 2\pi/\lambda_\phi) = \sqrt{AB}, \quad \alpha = \sqrt{A/B}$$

with

$$A = -(2\pi/\lambda) (m_0 c^2 \eta_s^3)^{-1},$$

$$B = eE_0 T \sin \phi_s.$$

The beam occupies an ellipse

$$\alpha^{-1}(\Delta\phi)^2 + \alpha(\Delta W)^2 = S.$$

The total number of phase oscillations,  $n_\phi$ , in each cavity ( $s = s_i$  to  $s_f$ ) is then

$$n_\phi = \int_{s_i}^{s_f} ds/\lambda_\phi(s).$$

Values of  $\alpha$ ,  $\lambda_\phi$  and  $n_\phi$  in each cavity are given in Table 1.

There are three effects which make the actual frequency different from  $\omega_\phi$ . (1) Coupling with the transverse motion. In the Lagrangian which describes the motion of a particle in a linac, the coupling effect is contained in terms of the form

$$(\underline{r}^2)^n (\Delta\phi)^m \quad n, m = 1, 2, \dots$$

where  $\underline{r}$  is the transverse coordinate of the particle. The oscillation frequency is increased by a factor (lowest order)

$$1 + (1/2)(\pi r/\eta_s \lambda)^2.$$

The effect is not very important, a few percent at the injection and less than one-half percent after 10 MeV. (2) Space charge forces.<sup>6</sup> In general, focusing action of the accelerating field is weakened by space charge forces and the oscillation frequency is 70%-80% of what is given in Table 1 when the beam intensity is of the order of 100 mA. Since the longitudinal space charge force depends strongly on beam sizes in all three directions, it is difficult to predict the total number of phase oscillations without detailed numerical

calculations. (3) Nonlinearity. The linear frequency  $\omega_\phi$  applies only for a small amplitude oscillation. For a larger amplitude ( $|\Delta\phi| \lesssim |\phi_s|$ ), the "instantaneous" frequency is approximately given by

$$\omega_\phi \left[ 1 - (\Delta\phi) / (2 |\tan(\phi_s)|) \right].$$

Thus the oscillation is slower ( $\Delta\phi > 0$ ) or faster ( $\Delta\phi < 0$ ) than the linear one and a spiral is introduced in the beam shape. If not corrected, this effect increases the final momentum spread more than (1) or (2).

#### SIMPLIFIED TREATMENT AND RESULTS

There have been many studies made on the beam dynamics in proton linacs, most of them quite elaborate requiring a use of large digital computers. The purpose of the present investigation is quite different from those. It was intended to be something useful and practical in the control room of a linac where there is a small digital computer for operating the linac. For example, at NAL, such a computer has been used not only for controlling the linac but also for obtaining the beam emittance. The calculation presented here is therefore based on the simplest possible approach. The transverse motion is entirely omitted and the velocity dependence of the transit time factor is ignored. For a high intensity beam, the calculation starts at a point where space charge effects are expected to be negligible. This means a certain beam

shape in the phase space is assumed at the end of the second or the third cavity as something beyond the control and the method is applied after that.

From the drift tube table of the linac, a simple interpolation formula is derived for the synchronous velocity in each cavity. The velocity is assumed to change abruptly at the center of each cell. Energy gain of the synchronous particle is then calculated and this is multiplied by  $\cos(\phi)/\cos(\phi_s)$  to find the energy gain for a nonsynchronous particle. The phase change from one gap to the next is simply

$$\delta(\Delta\phi) = (2\pi)(\beta_s - \beta)/\beta$$

since velocities  $\beta_s$  and  $\beta$  are assumed to be constant between the two gaps. Similarly, the effect of a drift space (length  $d$ ) between two cavities is

$$\delta(\Delta\phi) = -(2\pi d/\lambda)(\Delta W/m_0 c^2 \eta_s^3).$$

With a minor change, the calculation is extended to cases in which the rf level is less than 85% of the design value so that there is no real synchronous phase (no stable area). The beam can be placed anywhere in the phase space by simply shifting the rf phase of a cavity relative to the previous one. However, a caution is required when  $\beta$  is much less than  $\beta_s$ . Phase of the accelerating field changes appreciably within a single gap for such a particle and the transit time factor becomes meaningless in the calculation of the energy gain.

Indeed, even very elaborate calculations reported previously are not much reliable for investigating the behavior of "lost" particles.

Because of the phase damping ( $\beta^{-1/2} \sim \beta^{-3/4}$ , depending on the amount of space charge effects), the phase motion is approximately linear after the first cavity (10.4 MeV) and the essential features of the nonlinearity can be seen at the end of the first cavity. Two curves are given in Fig. 1; the solid curve is for a "d.c." beam at the injection (750 keV) and the dashed curve for a bunched beam, both at the end of the first cavity. The buncher voltage is 22.5 kV and its distance to the linac is 88.7 cm. Relative phases  $\Delta\phi$  at the first gap (for the solid curve) or at the buncher (for the dashed curve) are also shown along these curves. Phase acceptances are  $\Delta\phi = -41.4^\circ$  to  $64^\circ$  (28%) and  $\Delta\phi = -114.6^\circ$  to  $132.1^\circ$  (69%), respectively. It is seen that the tails of these two curves are almost identical so that, if one considers the entire beam, there will be no difference in the final momentum spread. It is, of course, advantageous to use a bunched beam since, in practice, one is interested in the momentum spread of, say, 95% of the beam. Under the normal condition, that is, if the beam is placed around the synchronous point in each cavity, its shape at the end of the linac is quite unfavorable as far as the momentum spread is concerned. This can be seen in Fig. 2 where the solid curve is

at the end of the linac (cavity No. 9) and the dashed curve is at the end of the cavity No. 8. Since the number of phase oscillations is close to one-quarter (see Table 1), the large phase spread ( $\sim 15^\circ$ ) of the dashed curve is converted to the large momentum spread of the solid curve. If the beam is shifted to the right, the oscillation frequency is smaller for particles on the right (large, positive  $\Delta\phi$ ) than on the left because of the nonlinearity. At the same time the number of oscillations becomes less than one quarter for the entire beam and the bunch may move in the phase space without rotating around its own center. On the other hand, if it is shifted too much to the right, part of the beam moves along "unstable" flow lines causing a large momentum spread. The oscillation frequency can also be controlled by changing the rf level in the last cavity. The dependence of the frequency on the accelerating field E is

$$\omega_\phi^2 \propto \sqrt{E^2 - E_0^2 \cos^2 \phi_s}; \quad E_0, \phi_s = \text{design value}$$

with the synchronous phase

$$\phi_s' = \cos^{-1}(E_0 \cos \phi_s / E).$$

Expected values of momentum spread are shown in Fig. 3 under different operating conditions of the last cavity. Central energy of the beam at the optimum point is different for different values of  $\phi_s'$  as indicated in the figure. However, the optimum value of  $\Delta p/p (\pm 0.8 \sim \pm 1.0 \times 10^{-3})$  is rather insensitive to the rf level and, although not shown here, the rf

level can be as low as ~60% of the design value. Note that below 85%, there is no synchronous phase and the motion is entirely "unstable." The expected shape of the momentum spectrum when  $E = E_0$  and the amount of beam shift =  $37.5^\circ$  is shown in Fig. 4. A beam size of  $\pm 1.5$  mm (which corresponds to  $\Delta p/p = \pm 0.5 \times 10^{-3}$ ) at the focal plane of an analyzing magnet is assumed in order to make a direct comparison with the measurement made by the linac group. The dashed curve in Fig. 4 is the result of a computer run\* using the program PARMILA.<sup>7</sup> Effects of transverse motions are included in the calculation with the invariant transverse beam quality of  $1.0 \pi$  mm-mrad. In general, transverse motion affects the final momentum spread only slightly ( $\leq 5\%$ ).

The scheme discussed here is applicable even when space charge effects are important. A computer program developed at Los Alamos, SCHEFF I,<sup>8</sup> has been used to find the beam shape at the end of cavity No. 8 for high intensity beams. When the intensity is 75 mA (design value of the NAL linac) and other parameters are identical to low intensity beams discussed above, 96% of the beam is contained within an ellipse

$$\gamma(\Delta\phi)^2 + 2\alpha(\Delta\phi)(\Delta W) + \beta(\Delta W)^2 = A$$

---

\*Computer runs with PARMILA have been made by W. Lee. His cooperation is greatly appreciated.

with

$$\alpha = 0.120 \text{ MeV/degree}, \quad \alpha = 0.882,$$

$$\beta = 14.82 \text{ degree/MeV and } A = 4.32 \text{ degree-MeV.}$$

Because of the space charge effect on the oscillation frequency, the orientation of the beam is different from the one shown in Fig. 2. Thirty points along the boundary of this ellipse have been traced in the last cavity using the simple procedure (no transverse motion, no space charge). Effects of shifting the beam relative to the rf phase in the cavity are shown in Fig. 5. It is interesting to see that again the optimum value,  $\Delta p/p \approx 1 \times 10^{-3}$ , is insensitive to the rf level. Results of the simple calculation given in Fig. 5 are generally in good agreement with SCHEFF runs that are continued to the end of the linac. Figs. 6-8 are typical examples of SCHEFF runs with  $E = E_0 (\phi'_s = -32^\circ)$ . One can see in Fig. 8 that the shift of  $35^\circ$  causes the right side of the beam to move down along unstable flow lines. The momentum spread will increase rapidly as the amount of shift is increased beyond this.

#### DISCUSSION

It is conceivable to design a multicavity linac taking into account a definite shape of the output beam. However, the shape is strongly dependent on other parameters (rf level, intercavity phase and the beam intensity) and a linac so

designed will be quite inflexible. Shifting of the beam relative to the rf phase of the last cavity seems to be the simplest way to control the momentum spread.

There are other possibilities of reducing the momentum spread which are somewhat more difficult. (1) Smaller synchronous phase angle in the first cavity. It is clear from Fig. 1 that, with or without a buncher, the tail part of the beam in the phase space makes a sizable contribution to the final momentum spread. A smaller synchronous phase ( $|\phi'_s| < 32^\circ$ ,  $E < E_0$ ) in the first cavity effectively rejects this part. However, since the lowest-order nonlinear term in the equation of phase oscillation is proportional to  $(\Delta\phi)/\tan|\phi'_s|$ , the distortion due to nonlinearity is not reduced. With  $\phi'_s = -20^\circ$ , the fraction of the bunched beam captured in the first cavity is 62% compared to 69% for  $-32^\circ$  so that the reduction in the beam intensity is 10%. If the beam is shifted properly in the last cavity, the final momentum spread becomes as small as  $\pm 0.6 \times 10^{-3}$  ( $\phi'_s = -40^\circ$ )  $\sim \pm 0.7 \times 10^{-3}$  ( $\phi'_s = -32^\circ$ ). One disadvantage of this scheme is the more stringent requirements on the rf level of the first cavity as well as on the relative phase between the buncher and the linac. For example, a drop of 5% in the rf level causes the synchronous phase to change from  $-32^\circ$  to  $-27^\circ$ , which is not too serious, but from  $-20^\circ$  to  $-8^\circ$  that will be disastrous. (2) Controlling the total number of

phase oscillation by changing the synchronous phase. The dependence of the oscillation frequency  $\omega_\phi$  on the synchronous phase  $\phi'_s$  is

$$\omega_\phi \propto \sqrt{E \sin|\phi'_s|} = \sqrt{E \cos \phi'_s} \sqrt{\tan|\phi'_s|}$$

where  $(E \cos \phi'_s)$  is a constant machine parameter. By raising or lowering rf levels in cavities, one can change the synchronous phase and therefore the total number of oscillations such that the beam comes out of the linac with a small momentum spread. Two examples are seen in Fig. 9, both for an initially unbunched beam. If  $\omega_\phi$  is to be increased substantially in a single cavity, the required increase in the rf level may not be realizable due to a limit in the available rf power. Also, the transverse defocusing action of the accelerating field (proportional to  $\sin|\phi'_s|$ ) will be increased. On the other hand, a drastic reduction in  $\omega_\phi$  in one cavity requires a very small value of  $|\phi'_s|$  and consequently a linear phase space area that may be too small to contain the beam. An adjustment involving 3-4 cavities seems unavoidable.

(3) Debunching of the beam around the unstable fixed point ( $\phi = -\phi_s$ ). Around the unstable fixed point,  $\phi = -\phi_s$ , the linear phase oscillation is represented by hyperbolas

$$\alpha^{-1}(\Delta\phi)^2 - \alpha(\Delta W)^2 = \text{constant}/\alpha, \quad \alpha = \sqrt{|A/B|}.$$

The magnitude of  $(\Delta\phi)$  and  $\Delta W$  grows exponentially,

$$(\Delta\phi), \quad (\Delta W) \sim \exp(\sqrt{|AB|}s).$$

A way to debunch high energy beams based on this has been discussed by L. Teng.<sup>9</sup> Although the emphasis is placed only on stretching the beam, the scheme may be useful for reducing the momentum spread as well. The beam is placed around the unstable point in the next to the last cavity. At the end of the cavity, the total phase spread of the beam is large,  $50^\circ$  for  $\phi'_S = -32^\circ$  and  $32^\circ$  for  $\phi'_S = -12^\circ$ . Two parameters, the amount of beam shift and the rf level in the last cavity, are then adjusted to make the final momentum spread as small as possible. Unfortunately, the last cavity of the NAL linac is too "long" for this scheme. The momentum spread is much larger than  $\pm 1 \times 10^{-3}$  either due to an excessive amount of the beam rotation in  $(\Delta\phi)-(\Delta W)$  space (when  $E > E_0$ ,  $|\phi'_S| > 32^\circ$ ) or due to a large nonlinear distortion of the beam (when  $E < E_0$ ,  $|\phi'_S| < 32^\circ$ ). If the last cavity were one-third of the actual length, this method would be ideal. Nevertheless, if space charge effects on the momentum spread are serious in the subsequent transport system, it may turn out to be the most favorable one because of the large beam size in the longitudinal direction. It should be remembered that the ultimate object is to have a small momentum spread in the beam injected into the booster but not necessarily in the beam at the end of the linac.

The dependence of the momentum spread on the relative phase between the last two cavities has been confirmed by many measurements at NAL. When all cavities are properly

adjusted, the best value is  $\Delta p/p = \pm 0.7 \times 10^{-3} \sim \pm 1.0 \times 10^{-3}$  at 20 mA. Uncertainties are mostly due to the beam size correction and a small background correction.

This work is a result of many discussions held between the linac group and the accelerator theory group. The kind cooperation of members of the linac group is greatly appreciated.

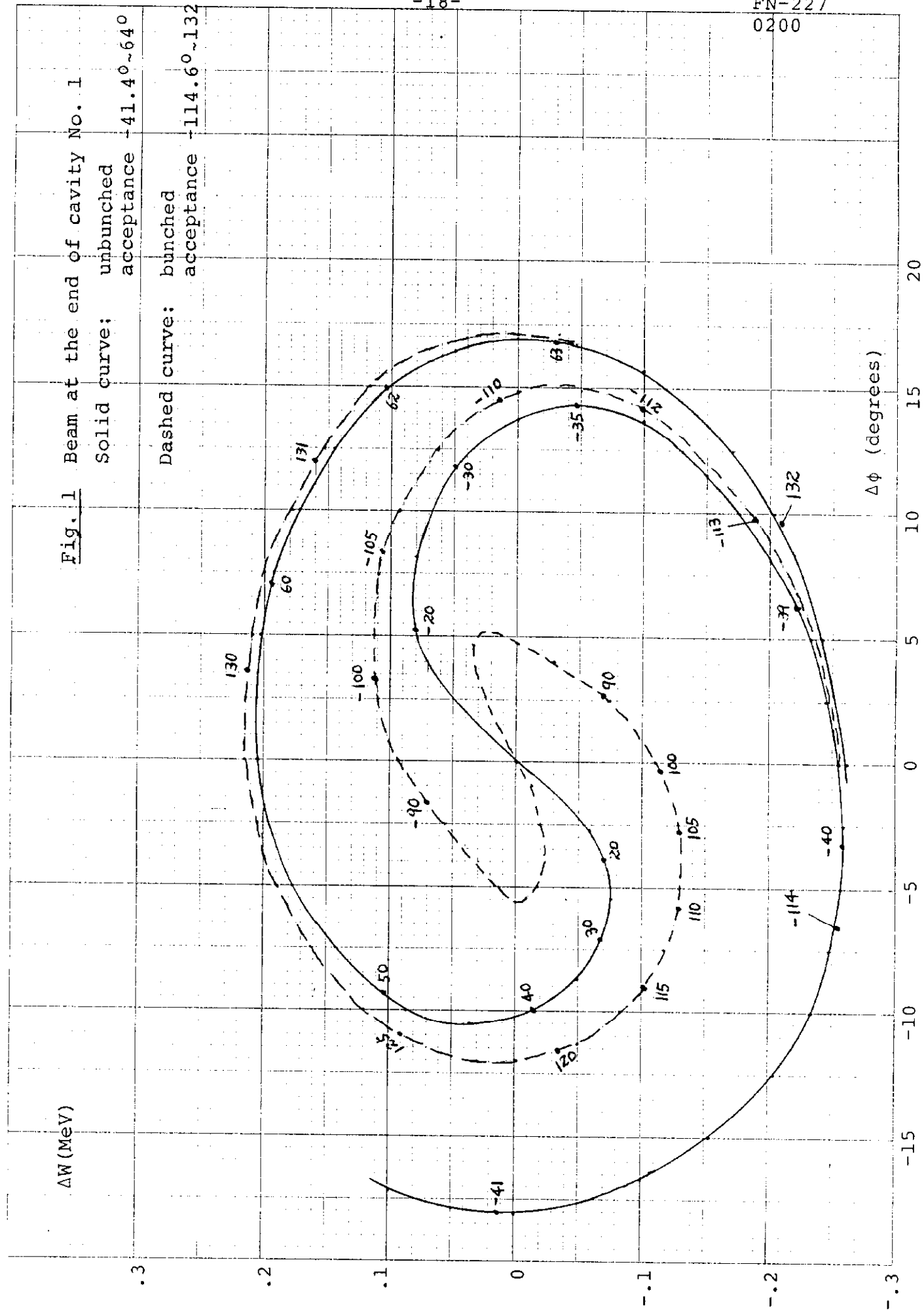
REFERENCES

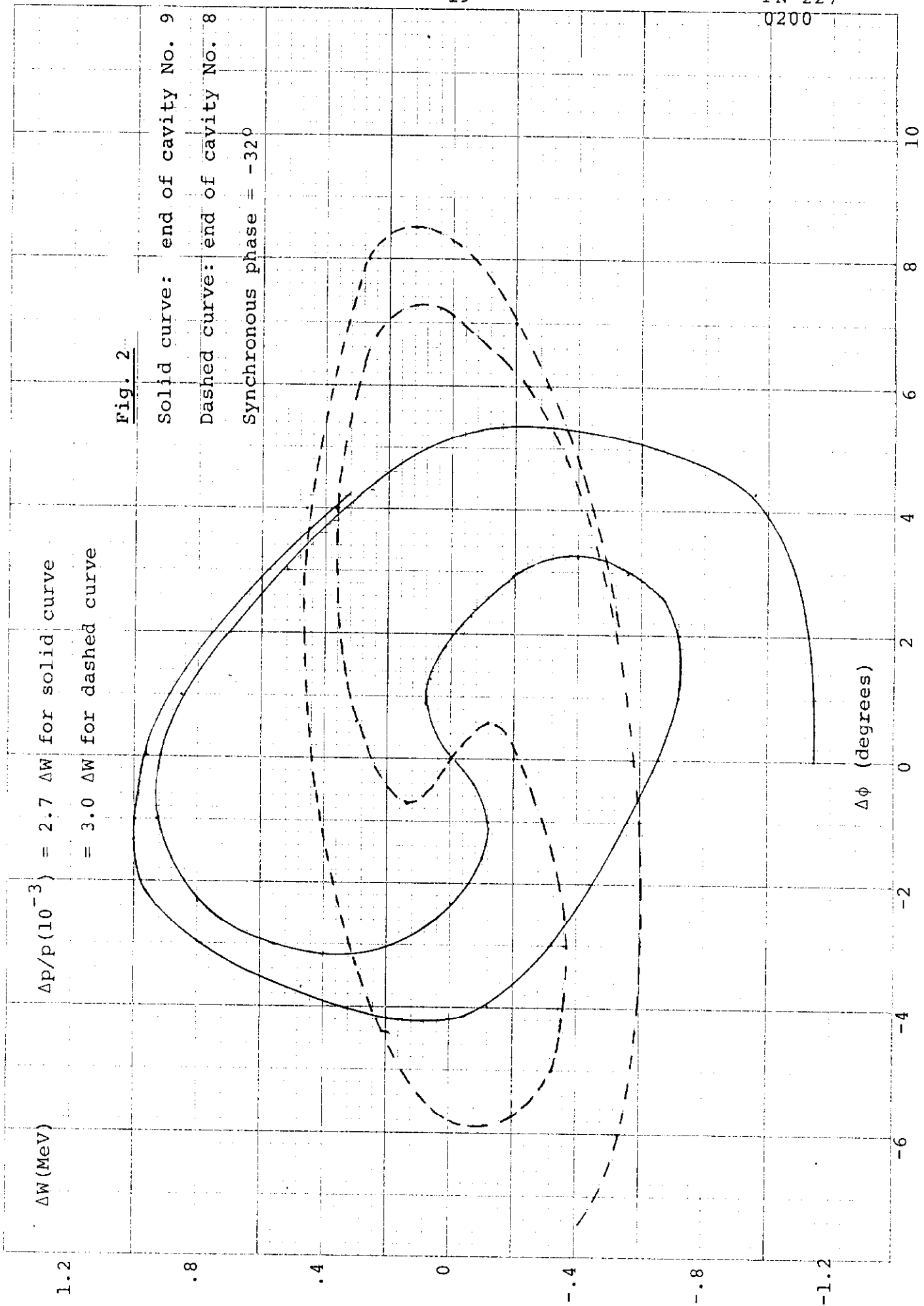
1. Design Report ("White Book"), National Accelerator Laboratory, July 1968, p. 9-26.
2. L. Smith, NAL Report FN-146, May 9, 1968.
3. Parameters for the NAL linac are given in C. D. Curtis et al., Particle Accelerator 1 (1970), 93.
4. R. L. Gluckstern, Proceedings of the 1966 Linear Accelerator Conference, Los Alamos Scientific Laboratory, p. 207; S. Ohnuma, ibid., p. 214.
5. S. Ohnuma, Yale Report Y-17, January 19, 1967.
6. R. L. Gluckstern, Linear Accelerators (edited by P. M. Lapostolle and A. L. Septier, North Holland, 1970), p. 827.
7. D. A. Swenson and J. E. Stovall, LASL Report No. MP-3-90 (1969).
8. J. E. Stovall, LASL Report MP-3-19 (1968).
9. L. C. Teng, Minutes of the Conference on Proton Linear Accelerators, Yale University, October 21-25, 1963, p. 49.

Table 1

CHARACTERISTIC PARAMETERS OF THE LINEAR  
PHASE OSCILLATION IN THE NAL LINAC

Cavity	Cell	Energy (MeV)	$\alpha$ (MeV <sup>-1</sup> )	$\lambda_{\phi}$ (m)
1	1	.78	10.80	1.019
	29	3.66	2.906	2.806
	56	10.25	1.189	5.411
number of linear oscillations = 2.68				
2	1	10.58	1.201	5.737
	31	22.41	.6858	10.19
	60	37.26	.4787	15.42
number of linear oscillations = 1.91				
3	1	37.91	.4091	13.53
	18	51.28	.3318	17.45
	35	65.74	.2807	21.67
number of linear oscillations = 0.953				
4	1	66.62	.2782	21.92
	29	92.09	.2254	29.44
number of linear oscillations = 0.654				
5	1	93.04	.2181	28.95
	24	116.0	.1894	35.63
number of linear oscillations = 0.484				
6	1	117.0	.1883	35.92
	22	138.5	.1696	42.30
number of linear oscillations = 0.398				
7	1	139.5	.1687	42.57
	21	160.0	.1552	48.85
number of linear oscillations = 0.347				
8	1	161.0	.1545	49.16
	20	180.5	.1444	55.28
number of linear oscillations = 0.304				
9	1	181.5	.1438	55.55
	19	199.8	.1361	61.52
number of linear oscillations = 0.269				
Total number of linear oscillations = 8.0				





$\Delta p/p$  (full width)

94% of the beam within  $\Delta p/p$

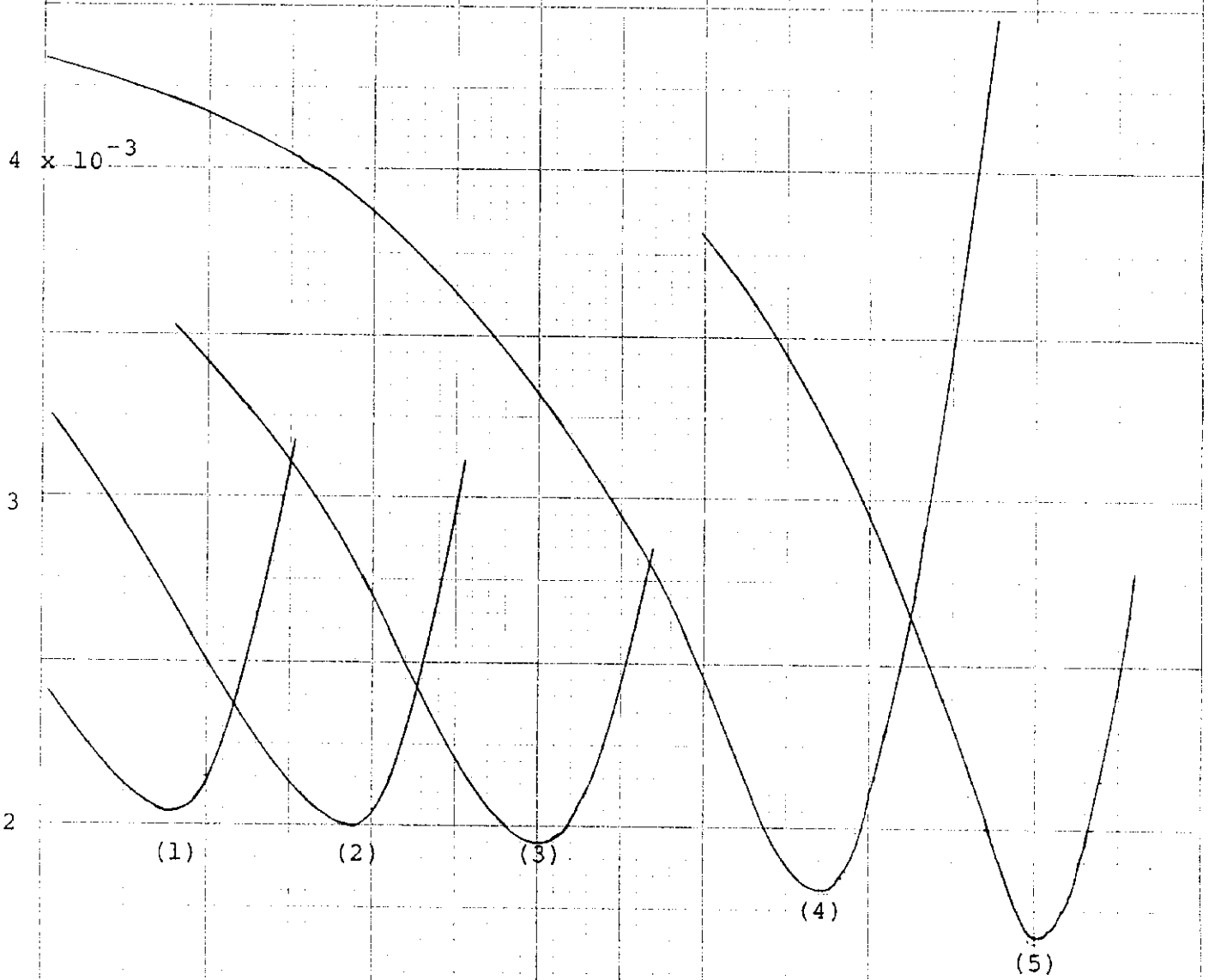


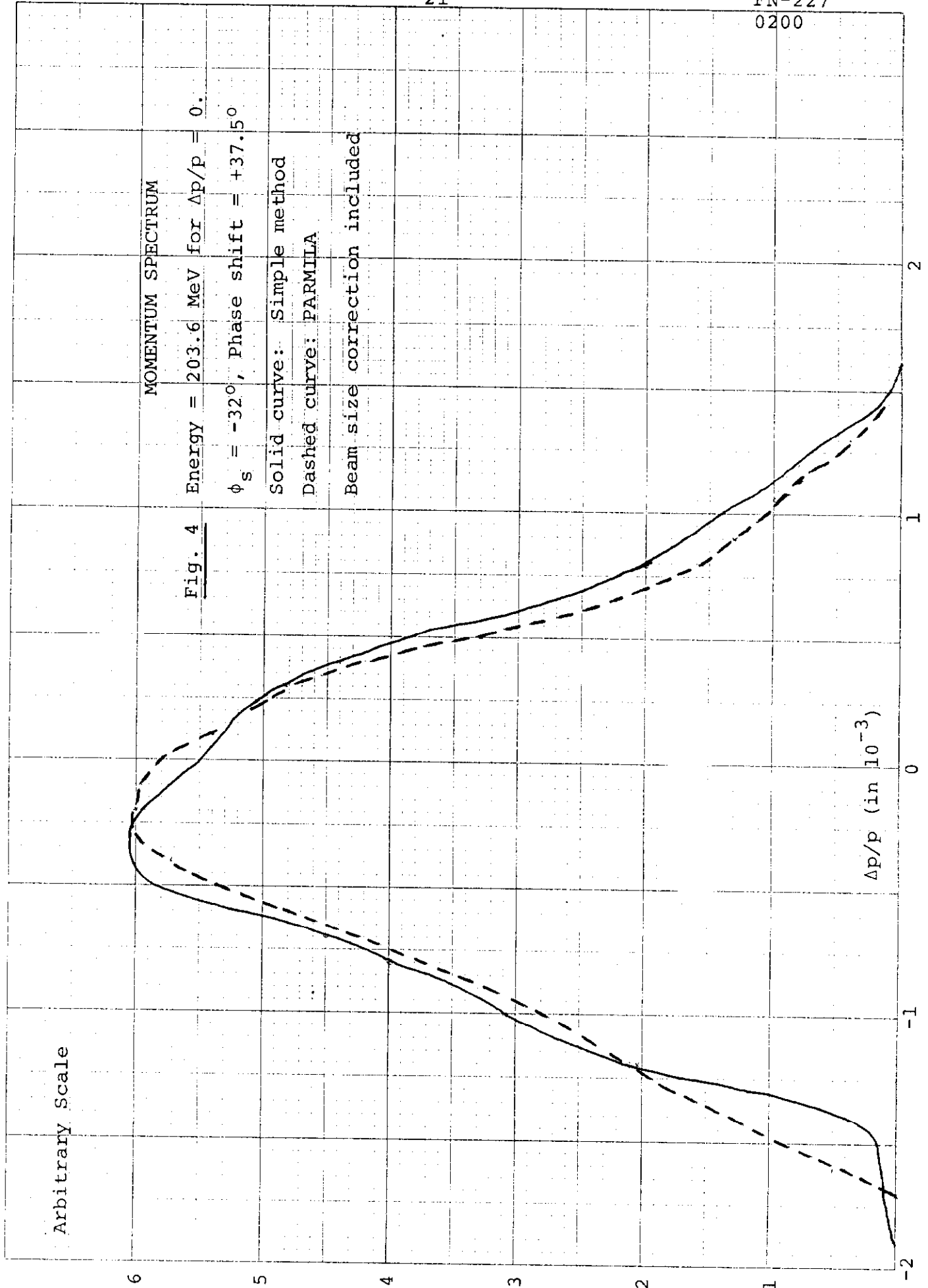
Fig. 3

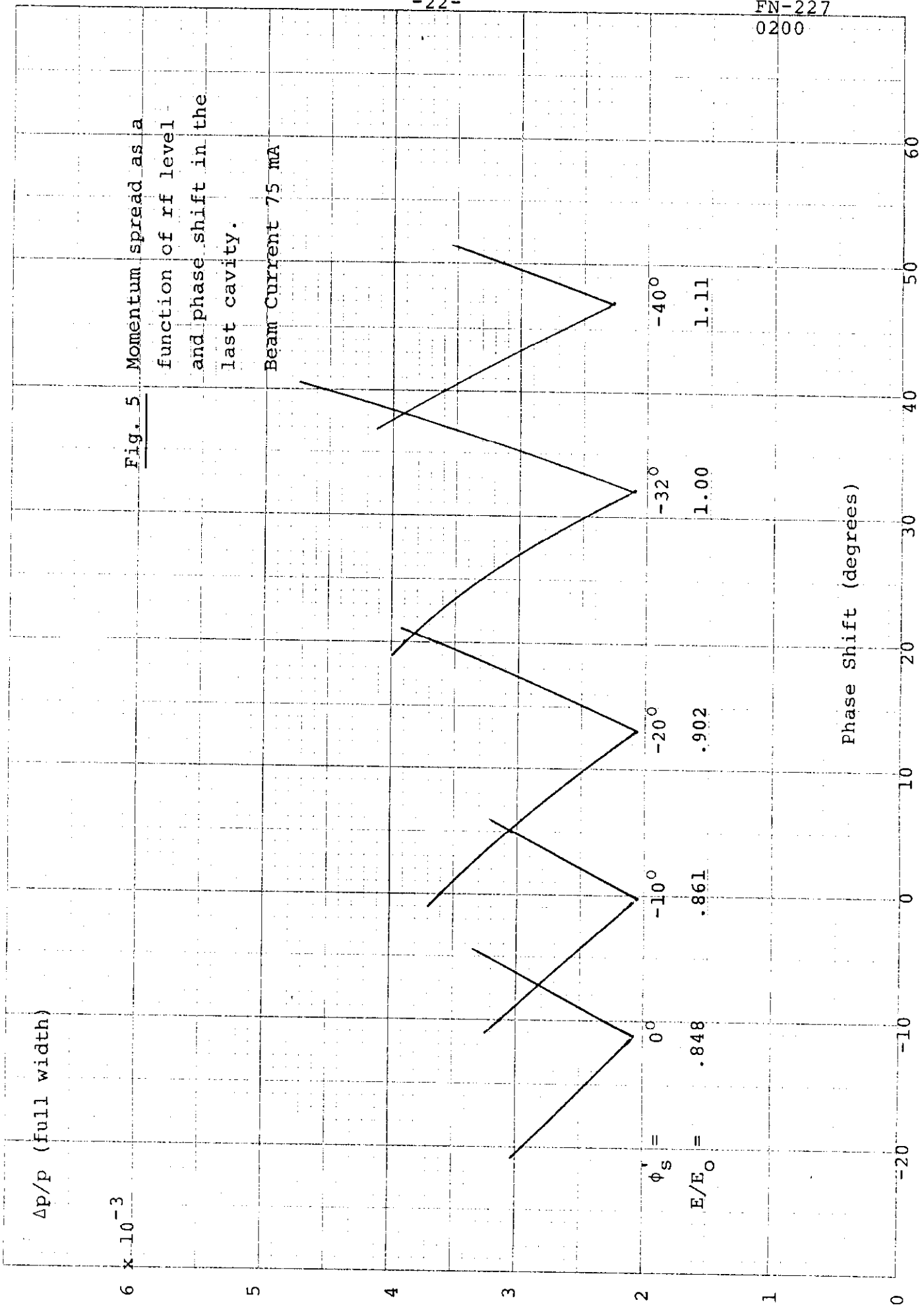
	(1)	(2)	(3)	(4)	(5)
$E/E_0$	.85	.86	.90	1.00	1.11
$\phi'_s$	0	-10	-20	-32	-40
$W_c$ (MeV)	200.3	200.6	201.5	203.6	205.7

$W_c$  = central energy of the beam at the minimum  $\Delta p/p$

Phase shift (degrees)

0 -10 0 10 20 30 40 50 60





OUTPUT AT END OF CELL NO.286

IF 20.0000

Fig. 6 SCHEFF I

Initially unbunched beam  
500 particles  
 $\phi_s = -320^\circ$  (All cavities)

No phase shift

$\Delta W = W - 200.2 \text{ MeV}$

$\Delta\phi$  (degrees)

-12      -8      -4      0      4      8      12      16

2.0000	I
1.9200	I
1.8400	I
1.7600	I
1.6800	I
1.6000	I
1.5200	I
1.4400	I
1.3600	I
1.2800	I
1.2000	I
1.1200	I
1.0400	I
0.9600	I
0.8800	I
0.8000	I
0.7200	I
0.6400	I
0.5600	I
0.4800	I
0.4000	I
0.3200	I
0.2400	I
0.1600	I
0.0800	I
0.0000	I
-0.0800	I
-0.1600	I
-0.2400	I
-0.3200	I
-0.4000	I
-0.4800	I
-0.5600	I
-0.6400	I
-0.7200	I
-0.8000	I
-0.8800	I
-0.9600	I
-1.0400	I
-1.1200	I
-1.2000	I
-1.2800	I
-1.3600	I
-1.4400	I
-1.5200	I
-1.6000	I
-1.6800	I
-1.7600	I
-1.8400	I
-1.9200	I
-2.0000	I

IF 20.0000

ORDINATE OF ABSISSA DPHI

Fig. 7 SCHEFF I

Initially unbunched beam  
500 particles  
 $\phi_s = -32^\circ$  (All cavities)

Phase shift =  $+30^\circ$

$\Delta W = W-203.2$  MeV

I = 20.0000

$\Delta W$ (MeV)

2.0000  
1.9200  
1.8400  
1.7500  
1.6800  
1.6000  
1.5200  
1.4400  
1.3600  
1.2800  
1.2000  
1.1200  
1.0400  
.9600  
.8800  
.8000  
.7200  
.6400  
.5600  
.4800  
.4000  
.3200  
.2400  
.1600  
.0800  
0.0000  
-.0800  
-.1600  
-.2400  
-.3200  
-.4000  
-.4800  
-.5600  
-.6400  
-.7200  
-.8000  
-.8800  
-.9600  
-1.0400  
-1.1200  
-1.2000  
-1.2800  
-1.3600  
-1.4400  
-1.5200  
-1.6000  
-1.6800  
-1.7600  
-1.8400  
-1.9200  
-2.0000

$\Delta\phi$  (degrees)

-12 -8 -4 0 4 8 12 16

ORDINATE OF ABSCISSA OF PHI

Fig. 8

SCHEFF I

Initially unbunched beam  
500 particles  
 $\phi_s = -32^\circ$  (All cavities)

Phase Shift =  $+35^\circ$

$\Delta W = W - 203.4 \text{ MeV}$

IF 20.0000

$\Delta W (\text{MeV})$

$\Delta\phi$  (degrees)

-16 -12 -8 -4 0 4 8 12 16

ORDINATE DE ABSCISSA DPHI

IF 20.0000

FN-227  
0200

